Hindawi
Mathematical Problems in Engineering
Volume 2018, Article ID 9398608, 8 pages
https://doi.org/10.1155/2018/9398608

Research Article

A Seven-Parameter BRDF Model with Double-Peak Characteristic Suitable for Sandy Soil

Yu-Feng Yang, Wen-Shuai Li, and Han-Zhi Zhang

School of Automation & Information Engineering, Xi'an University of Technology, Xi'an 710048, China

Correspondence should be addressed to Wen-Shuai Li; li.wen.shuai@icloud.com

Received 5 June 2018; Revised 29 August 2018; Accepted 18 October 2018; Published 29 October 2018

Academic Editor: Ana C. Teodoro

A seven-parameter BRDF model with double-peak characteristic was proposed in this paper, which can fit double-peak data. The global genetic algorithm was used to model the BRDF experimental data of sandy soil, and the parameter values and relative mean square error of the seven-parameter BRDF model were obtained. The results proved the correctness of the model, and the relative mean square errors of this model are, respectively, 0.30%, 0.22%, 0.26%, and 0.25% corresponding to the incident angles of 15°, 30°, 45°, and 60°. Additionally, we also combined data from four incident angles to derive seven parameters, which do not depend on incident angle, and the overall error is 1.79%. Finally, in order to intuitively show the BRDF of sandy soil, 3D BRDF graph of sandy soil with different incident angles is, respectively, given. It will be of great significance in practical project applications.

1. Introduction

Bidirectional Reflectance Distribution Function (BRDF) has been widely used in the fields of agricultural remote sensing, atmospheric radiation transmission, spectral scattering characteristics of rough surface targets, and material diagnosis [1–3]. In the fields of agricultural remote sensing and digital agriculture, BRDF is used to study the spatial distribution characteristics and spectral characteristics of the reflected light of object, as shown in Figure 1. Through measuring BRDF of crop leaves, crop growth parameters can be accurately characterized and quantitatively analyzed. So it has great advantages for researches and applications in the fields of vegetation remote sensing, agriculture, etc. [4, 5]. In recent years, the measurement and reproduction of the entire appearance of an object are one of the most important research directions in the field of color vision, and they are also one of the main application directions of BRDF. The use of BRDF to measure and model the surface appearance of reflective objects is a new method for entire appearance description, which has a very good development prospect [6]. In two-dimensional imaging, by method of BRDF the spectral and geometric characteristics of objects in a three-dimensional space can be captured, and the texture and color of the object surface are acquired, then under the required conditions the objects can be faithfully reproduced. Compared with traditional digital imaging, two-dimensional BRDF imaging can better reflect the interaction among observers, artworks, lighting, etc., in which it has its unique advantages [7]. In addition, environmental issues have become increasingly prominent in society. BRDF is also commonly used to measure the atmospheric environmental quality in a certain area. According to GOCIL1B data and solar zenith angle, combined with dark pixel method and 6S atmospheric radiation transmission model, area surface reflectance in typical weather can be inverted and accurately verified by using MODIS data [8, 9]. Since the reflection of visible light is different on the different materials surface, the use of BRDF to derive an effective light model is also the basis for the three-dimensional reconstruction [10, 11]. So it can be seen that BRDF has been widely used in aspects of society and the researches on it has become increasingly important.

In 2012, Yang Yufeng et al. combined a Minnaert model with a five-parameter semiempirical model to propose a six-parameter semiempirical model that satisfies the principle of conservation of energy and reciprocity under certain conditions [12–14]. The model has a good effect on the target with weak scattering characteristics. In the same year, Bai Lu

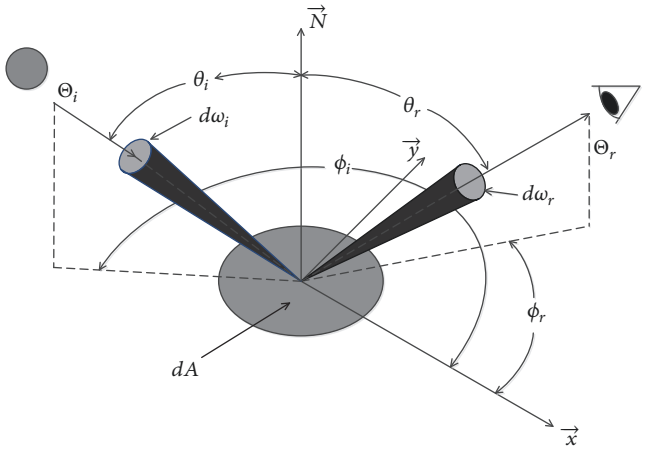

Figure 1: BRDF schematic diagram.

Figure 2: Sandy soil sample.

Figure 3: REFLET system.

et al. [15] combined the advantages of the 14-parameter model proposed by Renhorn et al. with the semiempirical BRDF statistical model and proposed a semiempirical statistical seven-parameter BRDF model with related theoretical foundations. The model adds two kinds of scattering to the five-parameter semiempirical statistical model; they are backscattering and bulk scattering, which improves the simulation accuracy of the surface with a smooth surface. In 2017, Liu Chenghao et al. [16] constructed a BRDF model based on deep neural network (DNN), which is suitable for space target material. It can be used to solve the limitation of describing the scattering properties of materials in BRDF empirical model and semiempirical model. In 2017, Zhang Ying et al. [17] established a dual Gaussian polarization BRDF model and simulated the model based on the microfacet model in order to more accurately describe the polarization BRDF of coating materials. To characterize the surface scattering polarization of coatings, Yang Min et al. [18] developed a multiparameter polarized BRDF model based on Kubelka-Munk theory, which is considered surface scattering and bulk scattering synthetically. The model characterizes the contribution of surface scattering by introducing a mirror coefficient to improve the traditional polarization-based BRDF model, which includes five parameters (real and imaginary parts of the complex refractive index, surface roughness, relative diffuse reflectivity coefficients, and mirror) and make the new polarization BRDF model consistent with the actual scattering polarization characteristics of the coating surface. However, these models are only for the specific practical application scenarios to innovate and optimize. But so far, most BRDF models can only fit the sample data which has single-peak, and it is difficult to accurately fit sample data with double peaks.

The study of soil bidirectional reflection characteristics has important significance for the development of quantitative remote sensing and soil remote sensing technology, which is the core of soil water content survey, surface temperature, surface albedo, etc. At the same time, it is also an important factor that must be considered in the global ground remote sensing research [19–25]. However, the BRDF data of soil commonly have double-peak characteristic, and most of the current BRDF models, such as Walthall empirical model, Hapke model, and SOMILSPECT model, have large errors in the fitting of the double-peak sample data, which poses a challenge to the existing BRDF models. In this paper, a seven-parameter BRDF model with double-peak characteristic was proposed and used to fit BRDF data with double peaks.

2. BRDF Seven-Parameter Statistical Model

The sandy soil sample is shown as Figure 2, whose particle size is less than 120μm, and the BRDF measurement experiments were entrusted to the 802 Institute in Shanghai that is specialized in BRDF data measurement for many years, which provided BRDF data. During the experiment, REFLET system, as shown in Figure 3, was used for BRDF measurement, which is a compact mechanized optical system produced by Light Tech of France for the detection of scattering properties of all materials and objects. It can quickly and easily measure the light distribution of illuminants or the spectral composition of the scattering lobes. And a complete description of the scattering properties in 3D space after light enters the surface can be fully described. The completion time of this experiment is June 5, 2017, and the quality of the measured data meets the experimental requirements.

Sandy soil BRDF usually has double peaks, as shown in Figure 4. The single-peak BRDF data only has a maximum value at a certain scattering angle, and the double-peak

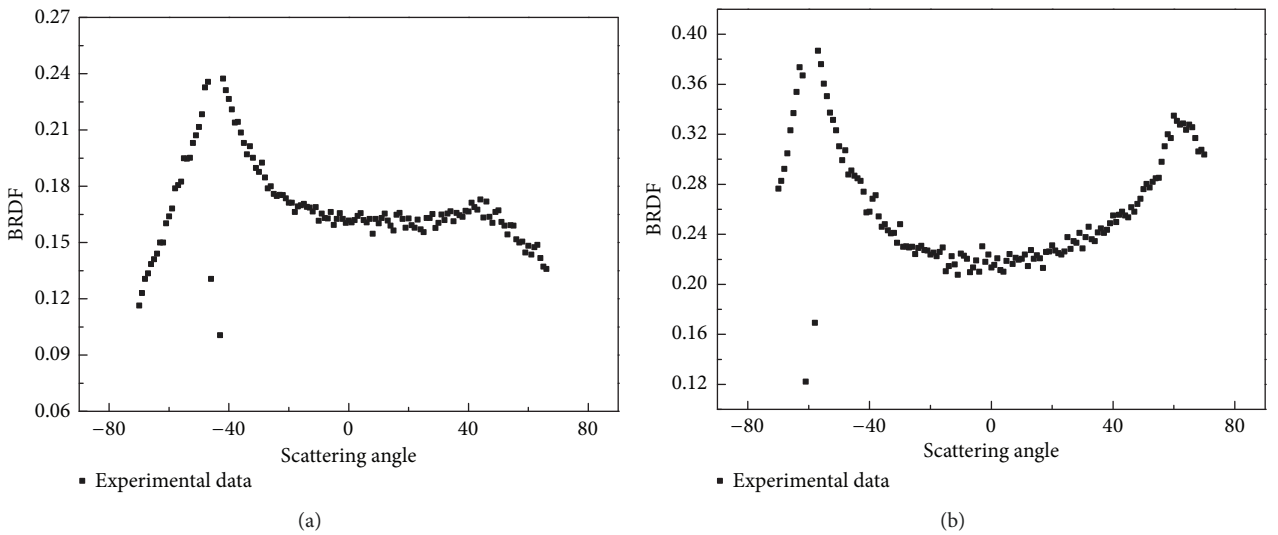

Figure 4: Sandy soil BRDF data with double-peak characteristic. (a) Sandy soil BRDF data of 30° incident zenith angle. (b) Sandy soil BRDF data of 60° incident zenith angle.

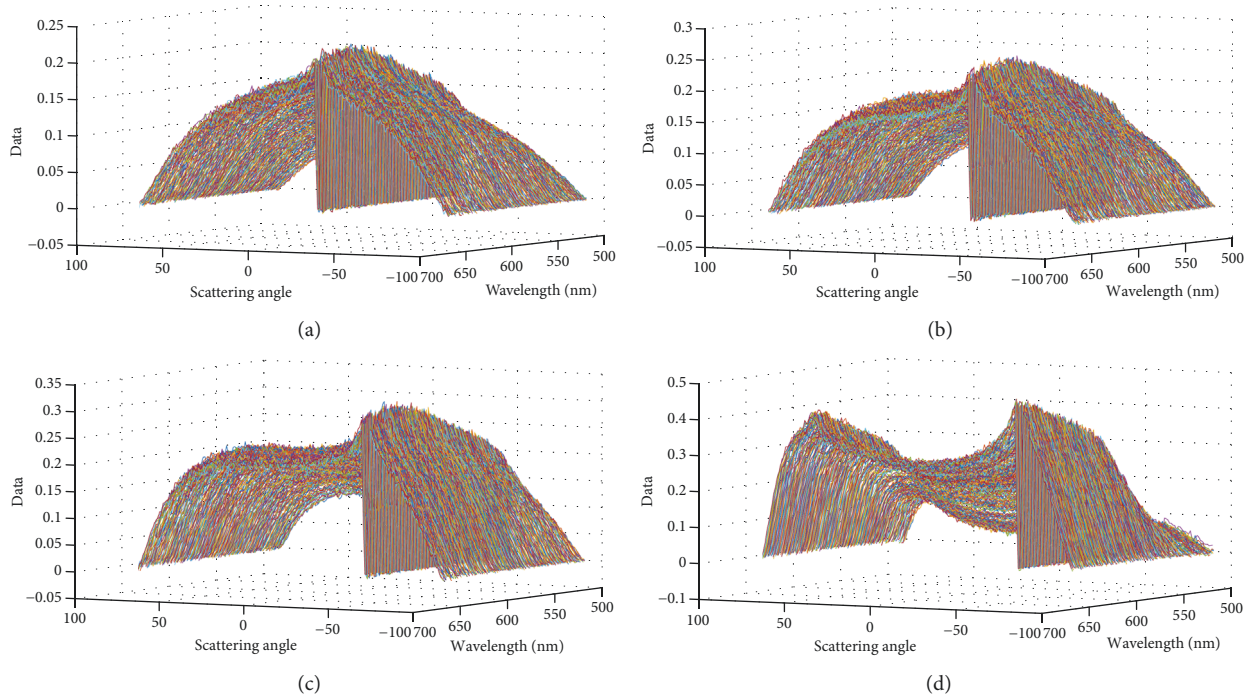

Figure 5: 3D graph of sandy soil BRDF data. (a) 15° incident zenith angle. (b) 30° incident zenith angle. (c) 45° incident zenith angle. (d) 60° incident zenith angle.

data has two peaks whose scattering angles are almost symmetrical. Due to the coincidence of the laser transmitter and receiver at a certain angle, the receiver does not receive a signal at this angle, the data show a few individual minimums at the certain angle, as shown in Figure 4.

Figure 5 shows the 3D data plot of the sandy soil sample with incident angles of 15°, 30°, 45°, and 60° (when incident angle is equal to 0°, there is only one peak at the scattering zenith angle of 0°; its form is simple. So the 3D graph of this angle is not given out). From Figure 5, it can be seen that, as the incident angle increases, the sandy soil BRDF data gradually shows the second peak. When the incident angle is 60°, two peaks can be clearly seen from Figure 5(d).

Based on above, we proposes a seven-parameter empirical BRDF model with double-peak characteristic suitable for sandy soil:

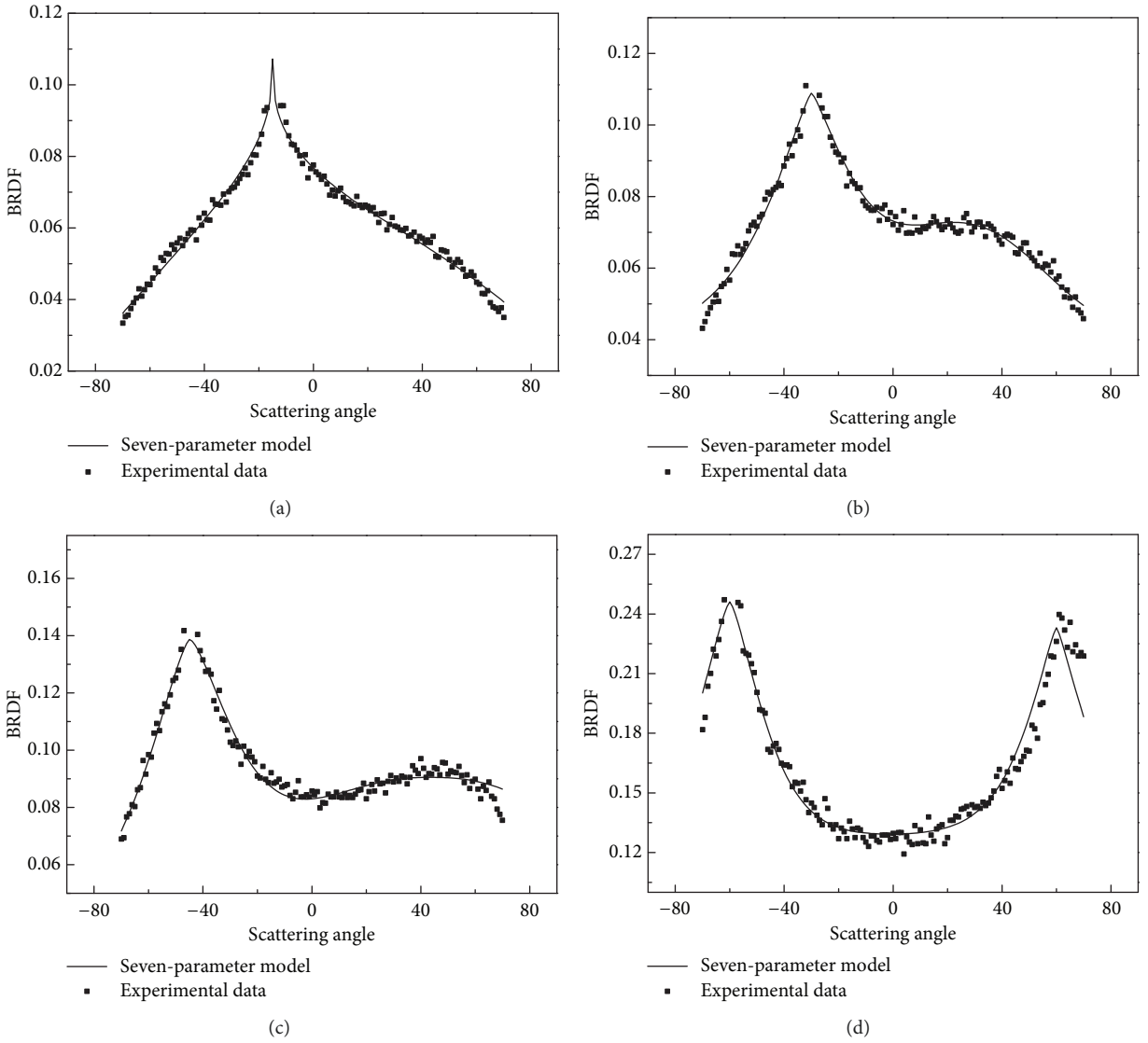

Figure 6: The fitting effects of the seven-parameter model for different incident zenith angles. (a) 15° incident zenith angle. (b) 30° incident zenith angle. (c) 45° incident zenith angle. (d) 60° incident zenith angle.

$$f_r(\theta_i, \theta_r, \phi_r) = k_a \exp\left[k_1 (1 - \cos\gamma_1)^a\right] + k_b \exp\left[k_2 (1 - \cos\gamma_2)^b\right] + \frac{k_c}{\cos\theta_i} \quad (1)$$

where

$$\cos^2\gamma_1 = \frac{\cos\theta_i \cos\theta_r - \sin\theta_i \sin\theta_r \cos(\phi_r - \phi_i) + 1}{2}$$
$$\cos^2\gamma_2 = \frac{\cos\theta_i \cos\theta_r + \sin\theta_i \sin\theta_r \cos(\phi_r - \phi_i) + 1}{2} \quad (2)$$

In (1), it is mainly divided into two parts. The first part represents the specular reflection component, and k_a, k_b are the mirror reflection coefficient. The second part represents the diffuse reflection component, and k_c is the diffuse reflection coefficient. $\exp[k_1(1 - \cos\gamma_1)^a]$ and $\exp[k_2(1 - \cos\gamma_2)^b]$represent reflection function, θ_i and θ_r, respectively, represent incident zenith angle and scattering zenith angle, ϕ_i and ϕ_r, respectively, represent incident azimuth angle and scattering azimuth angle, and k_a, k_1, a, k_b, k_2, b, and k_c are the parameters to be determined.

3. Seven-Parameter BRDF Model Validation

In order to verify the correctness of the model, seven-parameter BRDF model is verified by BRDF measured data of some sandy soil sample, in which the global genetic algorithm is used. Then we use MATLAB to fit the model to the data and perform error analysis on the model based on the relative mean square error. Because the BRDF value is small, the absolute error does not make sense, so we choose the relative mean square error here. The relative mean square error formula is as follows:

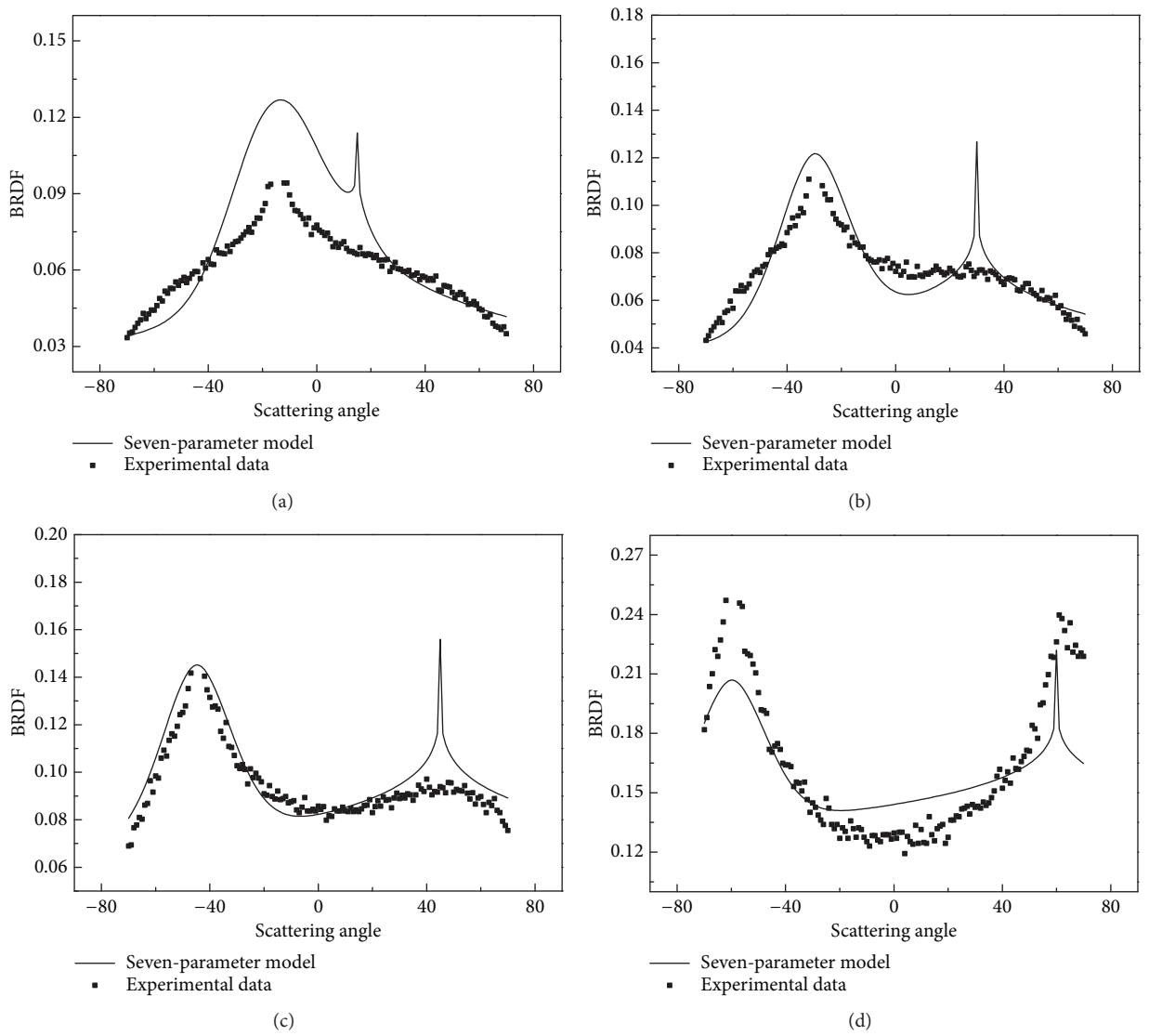

Figure 7: The fitting effects of the seven-parameter model with a fixed set of parameters for different incident zenith angles. (a) 15° incident zenith angle. (b) 30° incident zenith angle. (c) 45° incident zenith angle. (d) 60° incident zenith angle.

$$E = \frac{\sum_{i=1}^{N} \left(y_{\text{model}} - y_{data}\right)^2}{\sum_{i=1}^{N} y^2{}_{data}} \tag{3}$$

In (3), N represents the total number of data, y_{data} represents the measured data, and y_{model} represents the value of the model fitting curve.

As shown in Table 1, we use a set of parameters to fit the data for each incident zenith angle.

In the following, we use the BRDF model to analyze BRDF experimental data of the sandy soil sample with the parameters in Table 1. There are four sets of data corresponding to four scattering zenith angles. We conduct error analysis on four sets of data, respectively. For computational convenience here, we remove individual minimums that occur at a certain angle due to coincidence of laser emitters and receivers.

Figure 6 shows BRDF experimental data of sandy soil sample and the fitting effect of the model. The wavelength is equal to 650nm and the incident zenith angles are, respectively, 15°, 30°, 45°, and 60°. As Figure 6 shows, the fitting effect of this model is very good, especially for BRDF experimental data with double peaks as shown in Figures 6(a), 6(b), 6(c), and 6(d), in which the error is only 0.30%, 0.22%, 0.26%, and 0.25%, respectively. It can be seen from Table 1 that the error in fitting the four groups of data is very small. But it can also be seen from Figure 6, as the incident angle increases, the sandy soil BRDF data gradually shows the second peak, and the value of the peaks are, respectively, 0.0965, 0.1104, 0.1406, 0.2495, and 0.2406.

According to the BRDF experimental data of four sets of scattering angle distributions at different incident angles in the incident surface, a large parameter range is set for the initial value of the parameter. When a set of better solutions is obtained, the solution is centered on this set of solutions. By narrowing down the original set of parameters

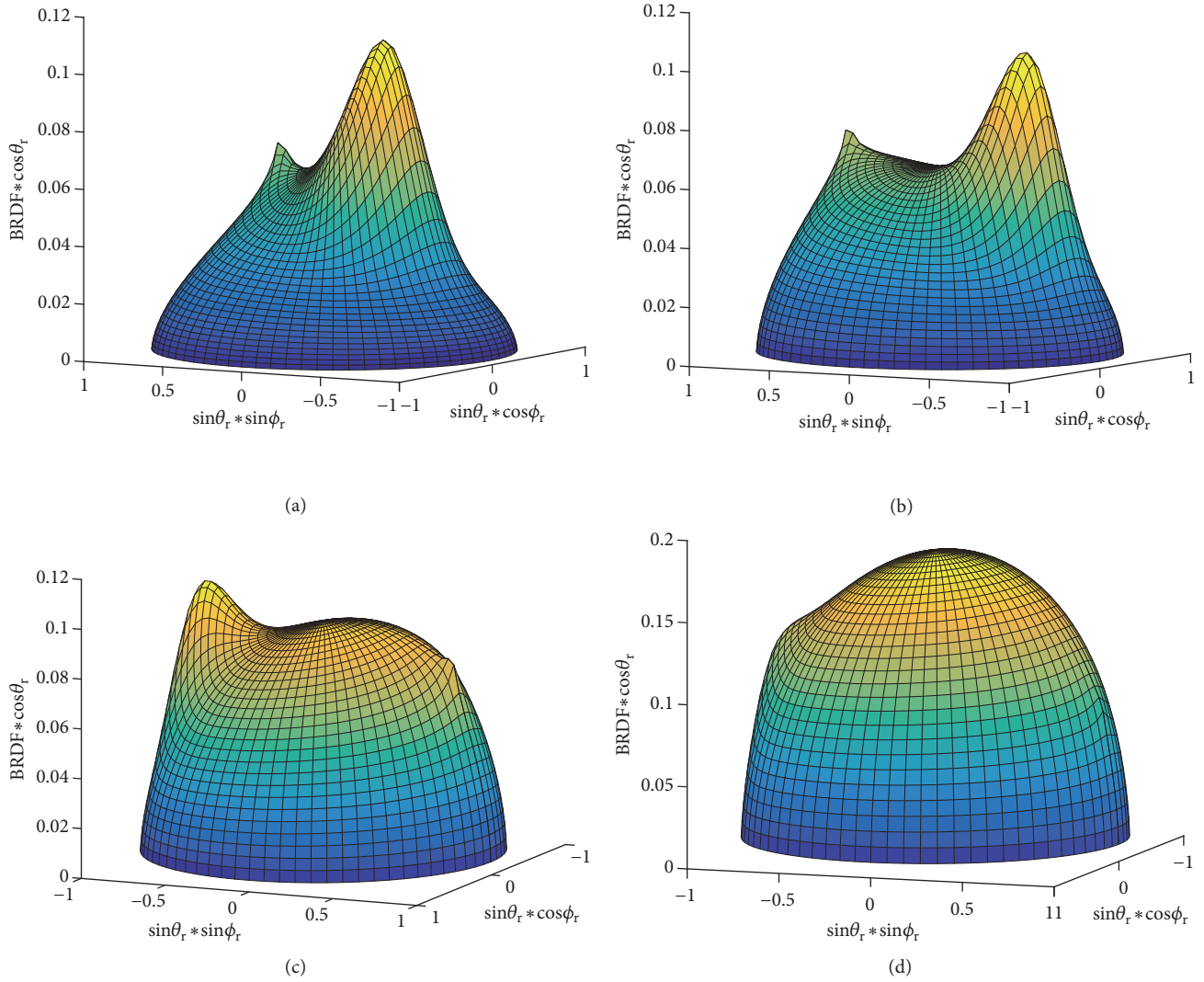

Figure 8: The fitting 3D graphs of sandy soil BRDF at 20°, 35°, 50°, and 65°. (a) 15° incident zenith angle. (b) 30° incident zenith angle. (c) 45° incident zenith angle. (d) 60° incident zenith angle.

Table 1: Model parameters and error for Figure 6.

	k_a	k_1	a	k_b	k_2	b	k_c	error
15°	-0.338	-0.2134	0.1805	0.0877	1.3467	1.2096	0.3479	0.30%
30°	0.0665	11.4655	0.6374	0.0289	21.3965	1.0363	0.0350	0.22%
45°	0.0688	47.9851	0.8908	0.0320	8.3861	1.6253	0.0402	0.26%
60°	0.1177	23.5580	0.6940	0.1047	18.8908	0.6322	0.0642	0.25%

Table 2: Model parameters and error for Figure 7.

	k_a	k_1	a	k_b	k_2	b	k_c	error	Overall error
(a)	0.0729	58.0301	0.9265	-0.0034	-3.3536	0.0273	0.1127	4.59%	1.79%
(b)								1.61%	
(c)								1.06%	
(d)								1.60%	

and repeating the calculation 2 to 3 times, it is basically possible to determine a set of general parameters suitable for different incident angles, as shown in Table 2, and the overall error is 1.79%.

As shown in Figure 7, this set of data also has a good fitting effect, especially for BRDF experimental data with double-peak characteristic; the seven-parameter BRDF model proposed in this paper can fit closer to the ideal near the peak.

Using the seven parameters derived, we can calculate the BRDF at any angle of incidence. In order to more clearly and intuitively represent the sandy soil BRDF, as shown in Figure 8, we draw out the fitting 3D graphs of sandy soil BRDF at 20°, 35°, 50°, and 65° using the seven general parameters we derived, which shows the fitting 3D graphs of sandy soil BRDF at different zenith angles. We can see that the seven general parameters have a good fitting effect at other angles, which shows that this set of data has wide adaptability.

4. Conclusion

In this paper a seven-parameter BRDF model is proposed that can fit double-peak BRDF data. With a sandy soil sample as an example, the correctness of the model is verified. As the increase of incident zenith angle, the sandy soil BRDF gradually shows double peaks. This model can overcome a common limitation of most previous models which cannot accurately fit double-peak data. In this paper, the global genetic algorithm is used to perform BRDF fitting analysis for the sandy soil BRDF data, and the corresponding parameter values and relative mean square error of the model are obtained. And the seven-parameter BRDF model can overcome the incapability of most of the current BRDF models, such as Walthall empirical model, Hapke model, and SOMILSPECT model, which also can fit very accurately. Finally, we combine data from four incident angles to derive seven parameters, which can give BRDF data of any angle by this seven-parameter BRDF model, not depending on incident angle.

Data Availability

The sandy soil BRDF data used to support the findings of this study were supplied by Institute in Shanghai and so cannot be made freely available.

Conflicts of Interest

The authors declare that there are no conflicts of interest regarding the publication of this article.

Acknowledgments

Thanks are due to Wang Biao in 802 Institute for doing data measurement for this study. This work was supported by the National Natural Science Foundation of China (61405157) and Natural Science Basic Research Plan in Shaanxi Province of China (2017JM6070).

References

[1] Y. Zhang, L. Jinlong, H. Zhiwei et al., "Research on Reflection and Phase Shift Characters of Metal Surface Based on BRDF Mode," *Electro-optic Technology Application*, vol. 32, no. 3, pp. 32–35, 2017.

[2] S. Dutta, S. K. Pal, and R. Sen, "Progressive tool flank wear monitoring by applying discrete wavelet transform on turned surface images," *J. Int. Meas. Confed*, vol. 77, pp. 388–401, 2016.

[3] Z. Wang et al., "Effect of surface roughness, wavelength, illumination, and viewing zenith angles on soil surface BRDF using an imaging BRDF approach," vol. 1161, 2016.

[4] F. Li, D. L. B. Jupp, M. Paget et al., "Improving BRDF normalisation for Landsat data using statistical relationships between MODIS BRDF shape and vegetation structure in the Australian continent," *Remote Sensing of Environment*, vol. 195, pp. 275–296, 2017.

[5] X.-Z. Zhang, P.-P. Du, Y. He, and H. Fang, "Review of Research and Application for Vegetation BRDF," *Guang Pu Xue Yu Guang Pu Fen Xi/Spectroscopy and Spectral Analysis*, vol. 37, no. 3, pp. 829–835, 2017.

[6] S. Lingnan, "Research on Appearance Reproduction of Object Surface Based on Bidirectional Reflectance Distribution Function," *Electro-Optic Technology Application*, vol. 2, 4, no. 28, pp. 10–15, 2013.

[7] Y. Weiye, *Research of image-based two-dimensional object BRDF*, Yunnan Normal University, 2013.

[8] A. Chappell, N. P. Webb, J. P. Guerschman et al., "Improving ground cover monitoring for wind erosion assessment using MODIS BRDF parameters," *Remote Sensing of Environment*, vol. 204, pp. 756–768, 2018.

[9] L. Yawen and L. Zhipeng, "Study on Atmospheric Correction of GOCI Data considering BRDF Model," *China Venture Capital*, vol. 26, 2017.

[10] H. Kumar, J. Ramkumar, and K. Venkatesh, "Surface texture evaluation using 3D reconstruction from images by parametric anisotropic BRDF," *Measurement*, vol. 125, pp. 612–633, 2018.

[11] L. Yongqing and A. Zhongqiang, "3D reconstruction lighting model," *Computer Knowledge and Technology*, vol. 16, pp. 167-168, 2015.

[12] Y. Cao, Z. Wu, H. Zhang, Q. Wei, and S. Wang, "Experimental Measurement and Modeling of Spectral Bidirectional Reflectance Distribution Function of Rough Target Specimen," *Acta Optica Sinica*, vol. 28, no. 4, pp. 792–798, 2008.

[13] Z. Hantao, W. Zhensen, and Z. Changmin, "Modeling and Comparison of BRDF with GA and GSAA," *Syetems Engineering and Electronics*, vol. 32, no. 7, pp. 1529–1533, 2010.

[14] Y. Yang, Z. Wu, and Y. Cao, "Practical six-parameter bidirectional reflectance distribution function model for rough surface," *Guangxue Xuebao/Acta Optica Sinica*, vol. 32, no. 2, 2012.

[15] L. Bai, Z. Wu, X. Zou, and Y. Cao, "Seven-parameter statistical model for BRDF in the UV band," *Optics Express*, vol. 20, no. 11, pp. 12085–12094, 2012.

[16] C. Liu, Z. Li, C. Xu, and Q. Tian, "BRDF Model for Commonly Used Materials of Space Targets Based on Deep Neural Network," *Guangxue Xuebao/Acta Optica Sinica*, vol. 37, no. 11, 2017.

[17] Y. Zhang, P. Song, and H. Zhao, "Double-Gauss polarimetric BRDF model of painted surfaces," *Hongwai yu Jiguang Gongcheng/Infrared and Laser Engineering*, vol. 46, no. 11, 2017.

[18] Y. Min, W. Jun, C. Fangxiao et al., "Multiple-Component Polarized Bidirectional Reflectance Distribution Function Model for Painted Surfaces Based on Kubelka-Munk Theory," *Acta Optica Sinica*, vol. 38, no. 1, 2018.

[19] C. Jiang and J. Song, "An Ultrahigh-Resolution Digital Image Sensor with Pixel Size of 50 nm by Vertical Nanorod Arrays," *Advanced Materials*, vol. 27, no. 30, pp. 4454–4460, 2015.

[20] F. Lu, X. Chen, I. Sato, and Y. Sato, "SymPS: BRDF Symmetry Guided Photometric Stereo for Shape and Light Source Estimation," *IEEE Transactions on Pattern Analysis and Machine Intelligence*, vol. 40, no. 1, pp. 221–234, 2018.

[21] M. Chandraker, "The Information Available to a Moving Observer on Shape with Unknown, Isotropic BRDFs," *IEEE Transactions on Pattern Analysis and Machine Intelligence*, vol. 38, no. 7, pp. 1283–1297, 2016.

[22] S. Cunming, S. Xiaobing, W. Han et al., "Model Optimization of Didirectional Polarization Reflectance Distribution Function of Land Surface Based on Airborne Polarimetric Data," *Journal of Atmospheric and Environmental Optics*, vol. 11, no. 2, pp. 125–133, 2016.

[23] Y. Liu, Z. Wang, Q. Sun et al., "Evaluation of the VIIRS BRDF, Albedo and NBAR products suite and an assessment of continuity with the long term MODIS record," *Remote Sensing of Environment*, vol. 201, pp. 256–274, 2017.

[24] H. Hao, B. Ye, and W. Zhensen, "BRDF Model of Bare Surface over Rugged Terrian," *Acta Optica Sinica*, vol. 1, pp. 266–273, 2016.

[25] C. K. Gatebe and M. D. King, "Airborne spectral BRDF of various surface types (ocean, vegetation, snow, desert, wetlands, cloud decks, smoke layers) for remote sensing applications," *Remote Sensing of Environment*, vol. 179, pp. 131–148, 2016.